Supplemental Materials

Molecular Biology of the Cell

Drechsler et al.

Supplementary Figure 1: *Figure supplement to Figure 1A*. **Peptide synthesis quality control.**ESI-MS (positive mode) spectra of synthesised modified peptides with cysteine. m/z – mass per charge in Dalton.

Supplementary Figure 2:*Figure supplement to Figure 1B and C*. (**A**) Extended panel showing a wider range of starPEG$(KA7)_4$ (*upper row*) bound to Atto647N-labelled microtubules (*lower row*). (**B**) High contrast versions of selected images shown in *Figure 1B and C*.

Supplementary Figure 3:*Figure supplement to Figures 1B and D*. **Ionic strength and pH-dependency of starPEG-$(KA7)_4$-TAMRA microtubule association.**Binding of starPEG-$(KA7)_4$-TAMRA to taxol stabilised Atto647N-labelled microtubules at the indicated ionic strength (*left block*) and pH (*right block*) conditions. Each picture pair shows tubulin (*left*) and starPEG-$(KA7)_4$-TAMRA (*right*) at the respective conditions given *on theleft* (ionic strength in mM or pH value) or by the exact buffer conditions *on the right* of each picture pair. *Graphs at the bottom* of each column depictthe starPEG-$(KA7)_4$-TAMRA intensity values per µm microtubule as a function of the ionic strength (*left*) or pH value (*right*). Averages of three independent flow channels (each 50-100 quantified microtubules) are shown. *Orange and purple lines* are exponential decay fits.

Supplementary Figure 4*: Figure supplement to Figure 1E.***Subtilisin treatment controls.**(**A**) 4-12% SDS-PAGE gel showing the non-treated (*left*) and the subtilisin-treated microtubule preparation (*right*) used for the binding-assay shown in Figure 1E. Proteins are indicated *on the right*, *subscript 's'* indicates subtilisin treated tubulin. Assignment according to (Alper et al., 2014). (**B**) starPEG-$(KA7)_4$-TAMRA (*mid and cyan in overlay on the right*) binding to (non-treated) brightly Atto647N-labelled GMP-CPP/taxol stabilised and dimly Atto647N-labelled GTP/taxol stabilised microtubules (*left and red in overlay on the right*). Arrowheads indicate bright GMP-CPP microtubules next to dim GTP microtubules, for easy comparison of bound starPEG-$(KA7)_4$-TAMRA.

Supplementary Figure 5:*Figure supplement to Figure 2 D and E.***Expansion of end-tracking starPEG-$(KA7)_4$-TAMRA onto the newly polymerised microtubule lattice after rescue.**(**A**) kymographs showing dynamic microtubules (*upper left*), associated starPEG-$(KA7)_4$-TAMRA (*lower left*), an intensity heatmap for bound starPEG-$(KA7)_4$-TAMRA (*upper right*) and a scheme indicating the behaviour of starPEG-$(KA7)_4$-TAMRA separated by rescue and catastrophe events (*lower right*). (**B**) (*left*) scheme indicating the parameters measured to calculate the graph on the (right). *Graph* showing the development of the starPEG-$(KA7)_4$-TAMRA intensity on the core microtubule (i.e., microtubule at the time of rescue, t=0s – *orangesquares and linear fit*), the microtubule extension (i.e., newly polymerised microtubule after rescue – *green circles and linear fit*), the total microtubule (i.e., core + extension, *magenta triangles and linear fit*) and on a starPEG-$(KA7)_4$-TAMRA (i.e., equilibrated control section >2µm distal to the plus end at t=0s – *black inverted triangle and linear fit*) as a function of the time after rescue (i.e., t=0s). Intensity values per µm microtubule were normalised to the core intensity at t=0s. Averages of 13 rescue events are shown. The slope ± standard error of the respective linear fits are given.

Supplementary Figure 6:*Figure supplement to Figure 4*. (**A**) Stills of Supplementary Movies 1.1-1.3 showing additional events of starPEG-$(KA7)_4$-TAMRA-mediated pulling of intersecting microtubules by depolymerising microtubule plus ends. In contrast to Figure 4A only the Alexa647-tubulin signal is shown, but now at 1s time resolution. Supplementary Movies 1.1 and 1.2 show examples for two consecutive pulling events by the same depolymerising microtubule. *Blue arrowheads* indicate the start of individual pulling events.(**B**) *Top panel row*: Stills showing the microtubule geometries during a starPEG-$(KA7)_4$-TAMRA-mediated pulling event. *White dashed box* indicates the area ('I') that is used in a 4-fold magnificationfor the overlay *on the bottom*, depicting the measurements made to calculate the bending forces that applied during pulling events (*please refer to'results' section for a detailed*

description). *Graph on the right* summarises calculated corrected bending forces for deflection angles ≤ 30º. *Horizontal bar* indicates median.

Supplementary Figure 7:*Figure supplement to Figure 5B*. Stills of Supplementary Movies 2.1-2.3 showing additional events of starPEG-$(KA7)_4$-TAMRA-mediated microtubule-zippering. In contrast to Figure 5B only the Alexa647-tubulin signal is shown, but now at 1s time resolution. *Blue arrowheads* indicate the interacting microtubules prior to bundling, *white arrowheads* the resulting overlaps.

Supplementary Figure 8: Schematics depicting possible applications for starPEG-$(KA7)_4$ derived constructs.*(***A***) Dynamic and reversible fluorescence-labelling of microtubules in vitro.* Microtubule labelling by starPEG-$(KA7)_4$ is robust, reversible and shows a good signal-to-noise ratio even in the presence of free tubulin due to a K_d in the low nanomolar range. At low concentrations, starPEG-$(KA7)_4$ can also be used in classical *in vitro* reconstitution experiments together with recombinant molecular motors or MAPs, as it does not significantly alter their behaviour on the microtubule lattice. StarPEG-$(KA7)_4$ can even be used to label dynamic microtubules with the caveats that i) microtubule growth rates are increased in its presence and ii) labelling of the growing plus end might be inefficient at lower starPEG-$(KA7)_4$ concentrations, as peptides are not able to track the growing end. For experiments that require a non-disturbed microtubule lattice, visualising microtubule by fluorescent starPEG-$(KA7)_4$ represents a good alternative to the stochastic covalent labelling of tubulin dimers with fluorescent dyes, which might result in lattice defects. In the current form, starPEG-$(KA7)_4$ is not suitable for *in vivo* applications, as it lacks selectivity towards other biomolecules with a negative surface charge (DNA, lipid bilayers) and cell permeability. (**B**) *Reversible physical and electrical screening of microtubules in vitro.* Our experiments further suggest that higher amounts of starPEG-$(KA7)_4$ on the microtubule lattice, impede the lattice association of motor proteins or the addition of tubulin dimers to the microtubule ends. Thus starPEG-$(KA7)_4$, could be used for (*in vitro*) applications that require to (reversibly) shield the microtubule lattice from physical or chemical interactions, selectively shut down lattice-dependent tubulin biology or to mask the negatively-charged microtubule lattice (fully decorated lattices are expected to be neutral to positively-charged). (**C**) *Targeting of modifying enzymes to the microtubule lattice in vitro.* starPEG-$(KA7)_4$ could be fused to any modifying enzyme of interest (e.g., kinases, phosphatases, acetylases, etc.) to target the enzyme to the microtubule lattice. Using non-tubulin-specific enzymes one could provoke non-natural modification patterns on the microtubule lattice. Fusing starPEG-$(KA7)_4$ to *bona fide* tubulin modifying enzymes might enhance their dwell time on the microtubule lattice thereby increasing the grade of modification. Translating the features of starPEG-$(KA7)_4$ into a linear geometry with protein (instead of PEG) linkers, this concept could be adopted for *in vivo* studies, probably provoking strong phenotypes that for example would facilitate examinations on the effect of posttranslational tubulin modifications on microtubule stability. (**D**) *Modifying the processivity of molecular motors*. Kinesins often feature a N-terminal extension preceding the actual motor domain. These extensions are involved in cargo binding (kinesin-3 (Gruneberg et al., 2006) and kinesin-7 (Drechsler et al., 2015; Roberts et al., 2014)), force generation (kinesin-1 (Khalil et al., 2008)) or microtubule association (kinesin-5 (Britto et al., 2016; Stock et al., 2003) and kinesin-7 (Drechsler et al., 2015)). In analogy to the kinesins-5 and -7, virtually any kinesin could be engineered with N-terminal or C-terminal (for minus end directed kinesins) $(KA)_n$ repeat extensions to increase their microtubule landing rates and processivity. This effect would be tuneable by the number of KA repeats and could convert non-processive kinesins, like kinesin-14, into highly processive ones. (**E**) *Microtubules as basis for plasmonic waveguides.* Microtubules self-assemble *in vitro* into stiff filaments with 25 nm diameter and several micrometre lengths. Given their high regularity on the nanoscale as well as the robustness and cost-effectiveness in their generation, microtubules are attractive candidates as template structures for material synthesis (Kirsch et al., 1997). Using starPEG-$(KA7)_4$ as linker, it will be conceivable to densely pack metal-nanoparticles onto the outer

surface of microtubules in pursuit of mass-producing functional nanostructures, such as plasmonic waveguides (Gür et al., 2016). (**F**) *Measuring depolymerisation-coupled pulling forces in vivo.* Magnetic beads coated with starPEG-$(KA7)_4$ that are injected into mitotic cells and moved by magnetic tweezers to the mitotic spindle midzone would eventually become attached to dynamic spindle microtubules. During depolymerisation phases, these beads would become end-on attached and could be used to measure *in vivo* microtubule-dependent depolymerisation-coupled pulling forces during metaphase and anaphase with a force-calibrated magnetic tweezer (Garzon-Coral et al., 2016).

Movie 1: Behaviour of starPEG-$(KA7)_4$-TAMRA (50nM) on dynamic microtubules. Please note the accumulationof starPEG-$(KA7)_4$-TAMRA on the microtubule lattice during depolymerisation indicated by an intensity increase of the TAMRA-signal.

Movie 2: Microtubule nucleation in the absence/presence of the indicated peptides at the given concentrations. Behaviour of starPEG-$(KA7)_4$-TAMRA (50nM) on dynamic microtubules. Please note that a rigor kinesin-1 mutant was used to immediately surface immobilise nucleated microtubules.

Movie 3: Collage of 3 movies (3.1-3.3) showing the depolymerisation coupled pulling of intersecting dynamic microtubules cross-linked by 50nM starPEG-$(KA7)_4$-TAMRA. *Left column* shows the starPEG-$(KA7)_4$-TAMRA signal only, the *column on the right* starPEG-$(KA7)_4$-TAMRA (*cyan*) superimposed on the tubulin signal (*red*). See also Figure 4 and Supplementary Movie 1.

Movie 4: Collage of 3 movies (4.1-4.3) showing bundling of dynamic microtubules by 50nM starPEG-$(KA7)_4$-TAMRA. *Left column* shows the starPEG-$(KA7)_4$-TAMRA signal only, the *column on the right* starPEG-$(KA7)_4$-TAMRA (*cyan*) superimposed on the tubulin signal (*red*). See also Figure 5 and Supplementary Movie 2. *Blue arrowheads* indicate microtubules before bundling, *white arrowheads* the final microtubule overlap.

Supplementary Movie 1: Collage of 3 movies (1.1-1.3) showing the depolymerisation coupled pulling of intersecting dynamic microtubules cross-linked by 50nM starPEG-$(KA7)_4$-TAMRA at a three-fold better time resolution as compared to Movie 3. Only the starPEG-$(KA7)_4$-TAMRA signal is shown. *Blue arrowheads and writing* indicate single pulling events. Please note that the same starPEG-$(KA7)_4$-TAMRA carrying depolymerising microtubule plus end can perform multiple sequential pulling events on different intersecting microtubules. See also Movie 3 and Supplementary Figure 6A.

Supplementary Movie 2: Collage of 3 movies (2.1-2.3) showing bundling of dynamic microtubules by 50nM starPEG-$(KA7)_4$-TAMRA at a three-fold better time resolution as compared to Movie 4. Only the starPEG-$(KA7)_4$-TAMRA signal is shown. *Blue arrowheads* indicate single zippering events, *white arrowheads* the final microtubule overlap. See also Movie 4 and Supplementary Figure 7.

Supplementary References

Alper, J.D., Decker, F., Agana, B., and Howard, J. (2014). The Motility of Axonemal Dynein Is Regulated by the Tubulin Code. Biophys J *107*, 2872-2880.

Britto, M., Goulet, A., Rizvi, S., von Loeffelholz, O., Moores, C.A., and Cross, R.A. (2016). Schizosaccharomyces pombe kinesin-5 switches direction using a steric blocking mechanism. Proceedings of the National Academy of Sciences *113*, E7483-E7489.

Drechsler, H., Tan, A.N., and Liakopoulos, D. (2015). Yeast GSK-3 kinase regulates astral microtubule function through phosphorylation of the microtubule-stabilizing kinesin Kip2. J Cell Sci *128*, 3910-3921.

Garzon-Coral, C., Fantana, H.A., and Howard, J. (2016). A force-generating machinery maintains the spindle at the cell center during mitosis. Science *352*, 1124-1127.

Gruneberg, U., Neef, R., Li, X., Chan, E.H.Y., Chalamalasetty, R.B., Nigg, E.A., and Barr, F.A. (2006). KIF14 and citron kinase act together to promote efficient cytokinesis. The Journal of Cell Biology *172*, 363-372.
Gür, F.N., Schwarz, F.W., Ye, J., Diez, S., and Schmidt, T.L. (2016). Toward Self-Assembled Plasmonic Devices: High-Yield Arrangement of Gold Nanoparticles on DNA Origami Templates. ACS Nano *10*, 5374-5382.
Khalil, A.S., Appleyard, D.C., Labno, A.K., Georges, A., Karplus, M., Belcher, A.M., Hwang, W., and Lang, M.J. (2008). Kinesin's cover-neck bundle folds forward to generate force. Proceedings of the National Academy of Sciences *105*, 19247-19252.
Kirsch, R., Mertig, M., Pompe, W., Wahl, R., Sadowski, G., Böhm, K.J., and Unger, E. (1997). Three-dimensional metallization of microtubules. Thin Solid Films *305*, 248-253.
Roberts, A.J., Goodman, B.S., and Reck-Peterson, S.L. (2014). Reconstitution of dynein transport to the microtubule plus end by kinesin. Elife *3*, e02641.
Stock, M.F., Chu, J., and Hackney, D.D. (2003). The Kinesin Family Member BimC Contains a Second Microtubule Binding Region Attached to the N terminus of the Motor Domain. J Biol Chem *278*, 52315-52322.

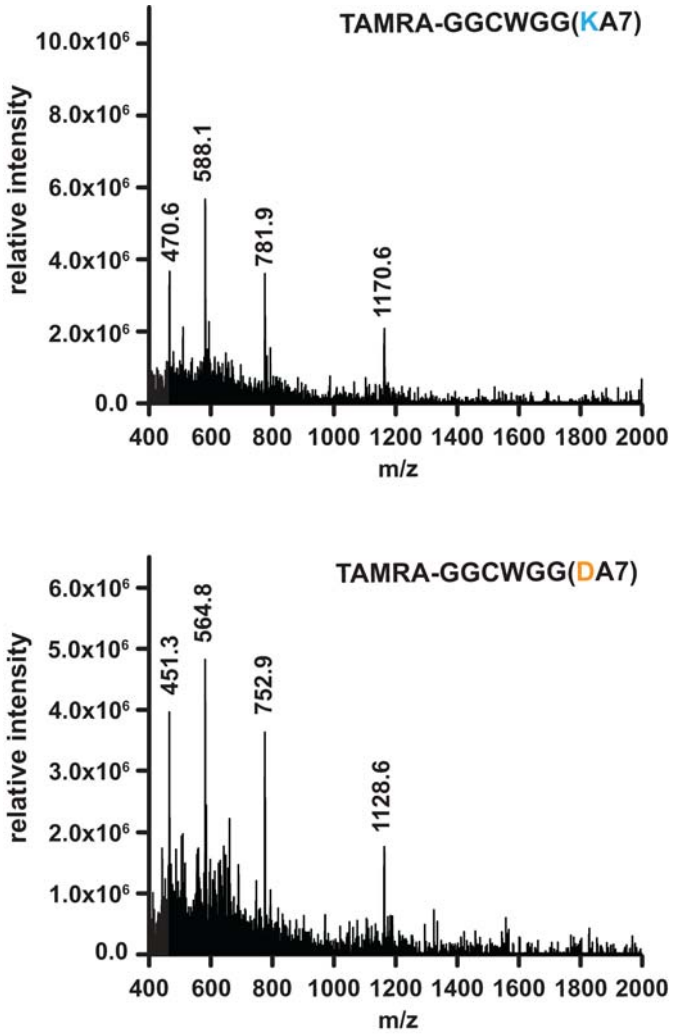
TAMRA-GGCWGG(KA7)
relative intensity
10.0x10⁶
8.0x10⁶
6.0x10⁶
4.0x10⁶
2.0x10⁶
0.0
470.6
588.1
781.9
1170.6
400 600 800 1000 1200 1400 1600 1800 2000
m/z
TAMRA-GGCWGG(DA7)
relative intensity
6.0x10⁶
5.0x10⁶
4.0x10⁶
3.0x10⁶
2.0x10⁶
1.0x10⁶
0.0
451.3
564.8
752.9
1128.6
400 600 800 1000 1200 1400 1600 1800 2000
m/z

Figure S1

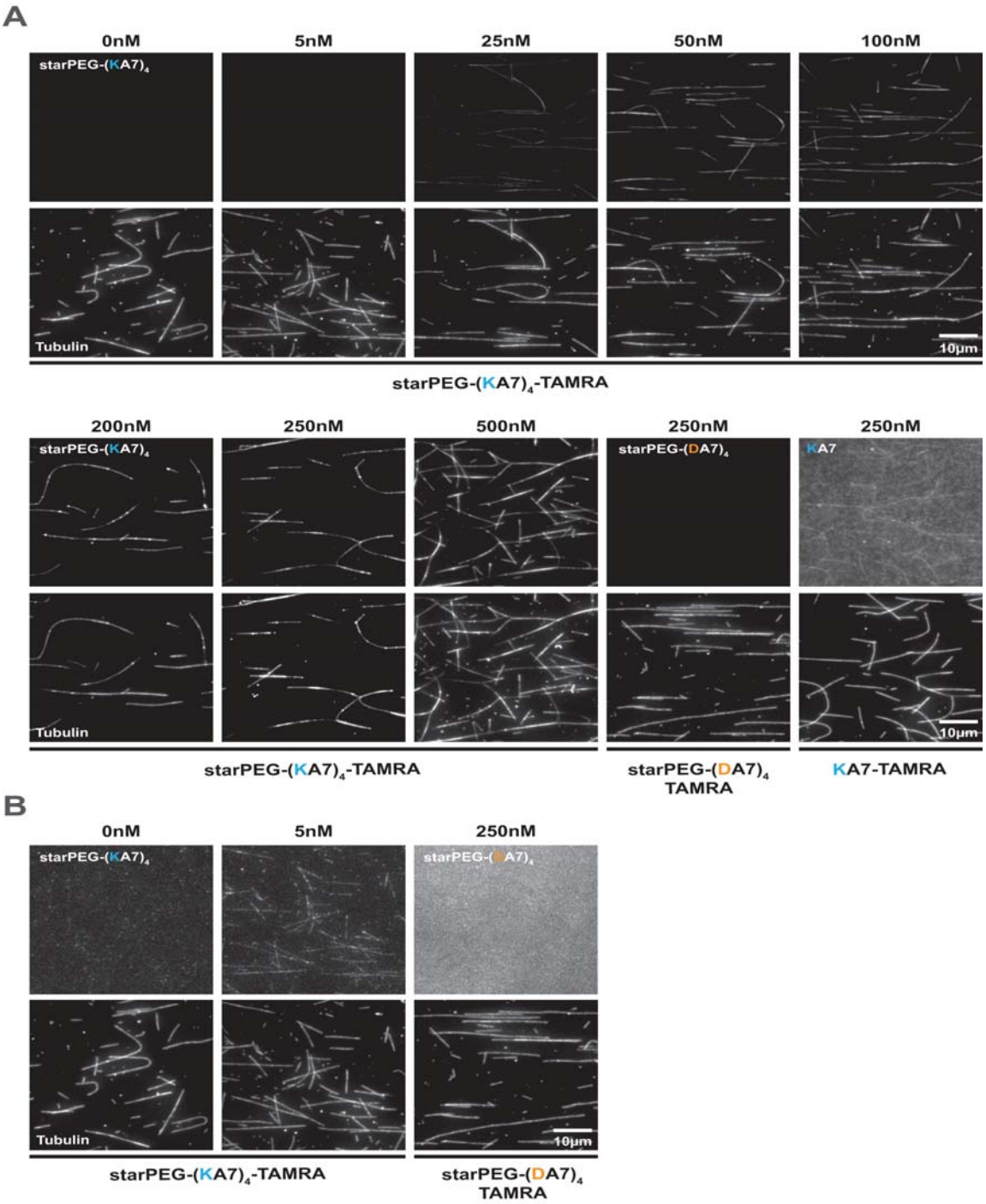
A
0nM
5nM
25nM
50nM
100nM
starPEG-(KA7)4
Tubulin
10μm
starPEG-(KA7)4-TAMRA
200nM
250nM
500nM
250nM
250nM
starPEG-(KA7)4
starPEG-(DA7)4
KA7
Tubulin
10μm
starPEG-(KA7)4-TAMRA
starPEG-(DA7)4 TAMRA
KA7-TAMRA
B
0nM
5nM
250nM
starPEG-(KA7)4
starPEG-(DA7)4
Tubulin
10μm
starPEG-(KA7)4-TAMRA
starPEG-(DA7)4 TAMRA

Figure S2

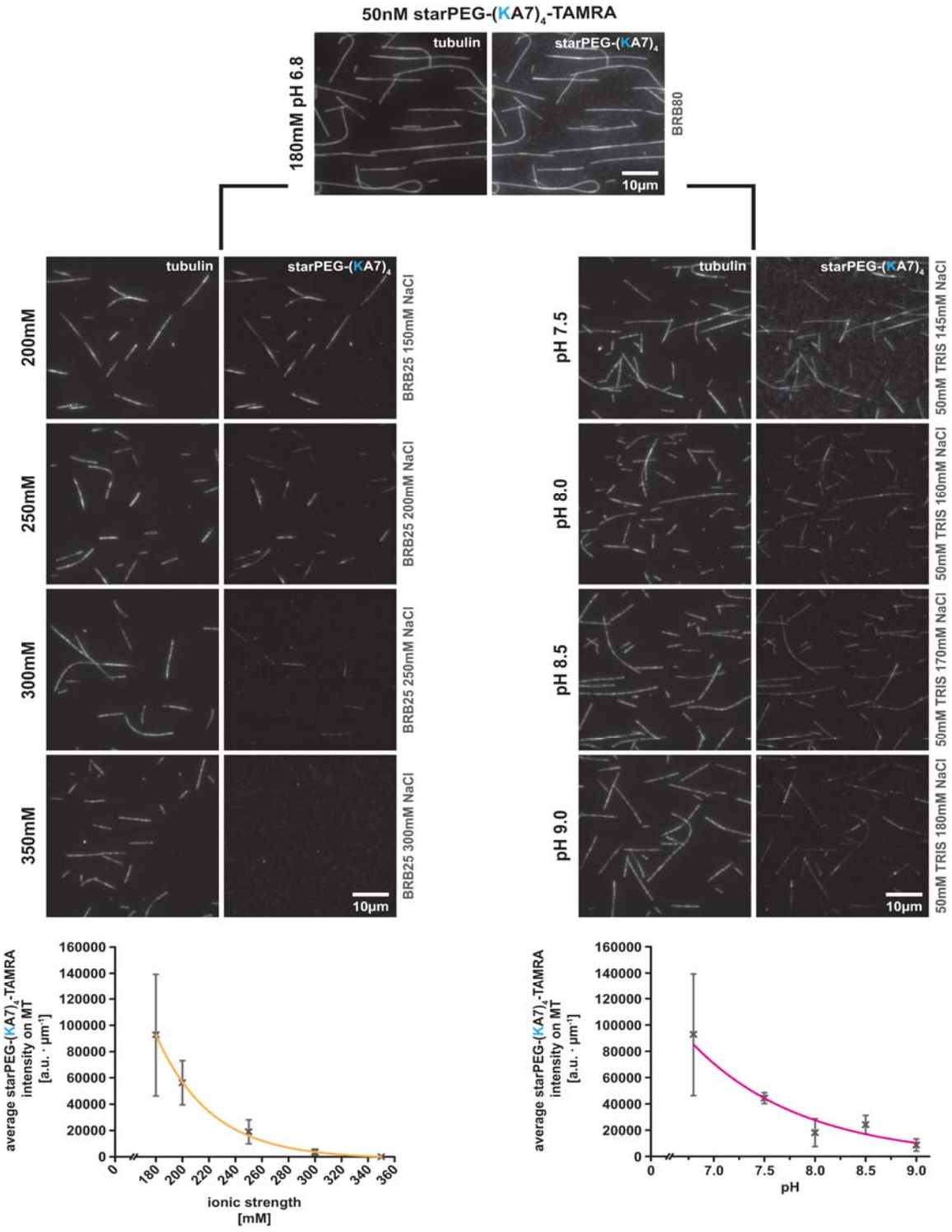
50nM starPEG-(KA7)4-TAMRA
180mM pH 6.8
tubulin
starPEG-(KA7)4
BRB80
10µm
200mM
250mM
300mM
350mM
BRB25 150mM NaCl
BRB25 200mM NaCl
BRB25 250mM NaCl
BRB25 300mM NaCl
pH 7.5
pH 8.0
pH 8.5
pH 9.0
50mM TRIS 145mM NaCl
50mM TRIS 160mM NaCl
50mM TRIS 170mM NaCl
50mM TRIS 180mM NaCl
average starPEG-(KA7)4-TAMRA intensity on MT [a.u. · µm-1]
ionic strength [mM]
pH

Figure S3

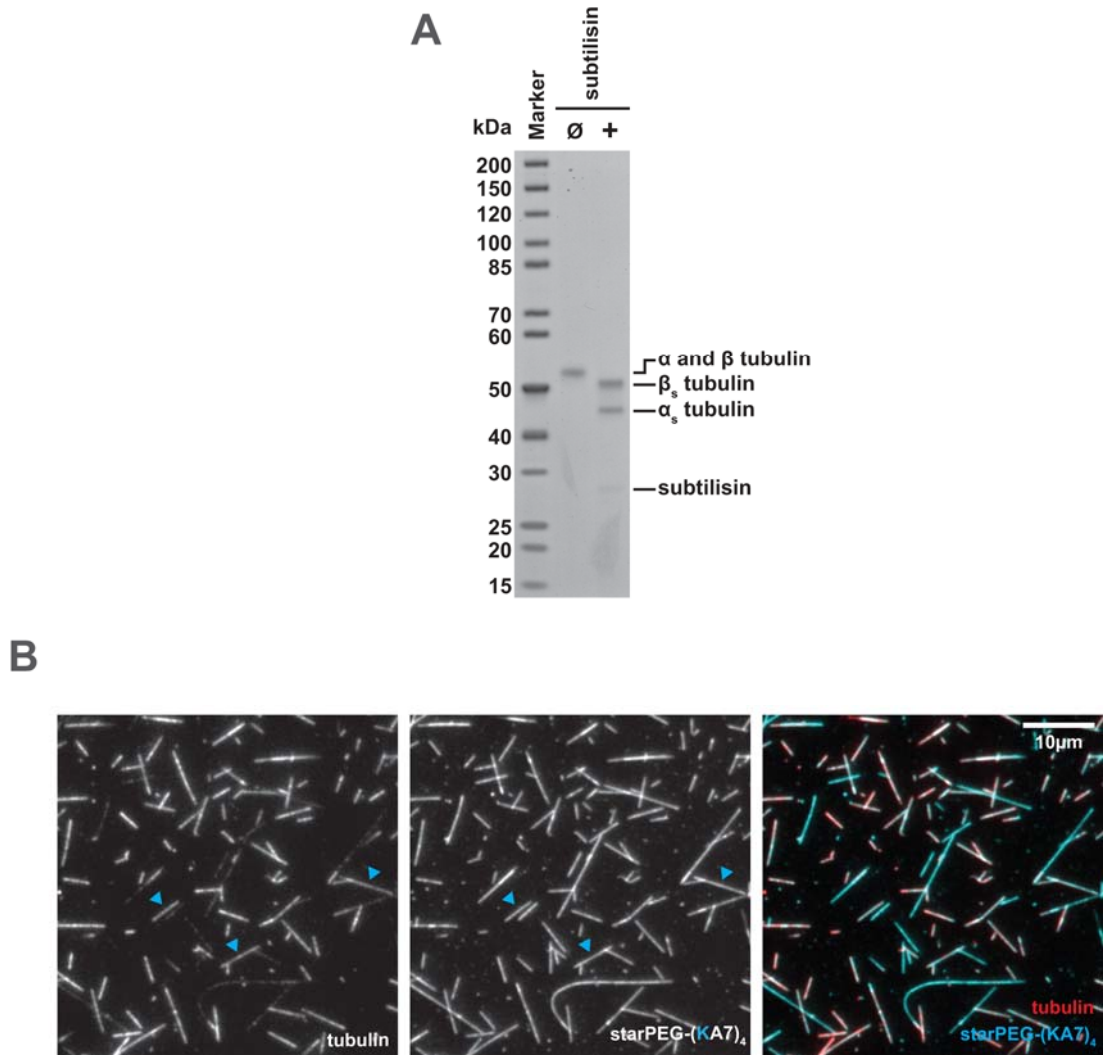
A
Marker
subtilisin
kDa
Ø
+
200
150
120
100
85
70
60
50
40
30
25
20
15
α and β tubulin
β$_s$ tubulin
α$_s$ tubulin
subtilisin
B
tubulin
starPEG-(KA7)$_4$
10µm
tubulin
starPEG-(KA7)$_4$

Figure S4

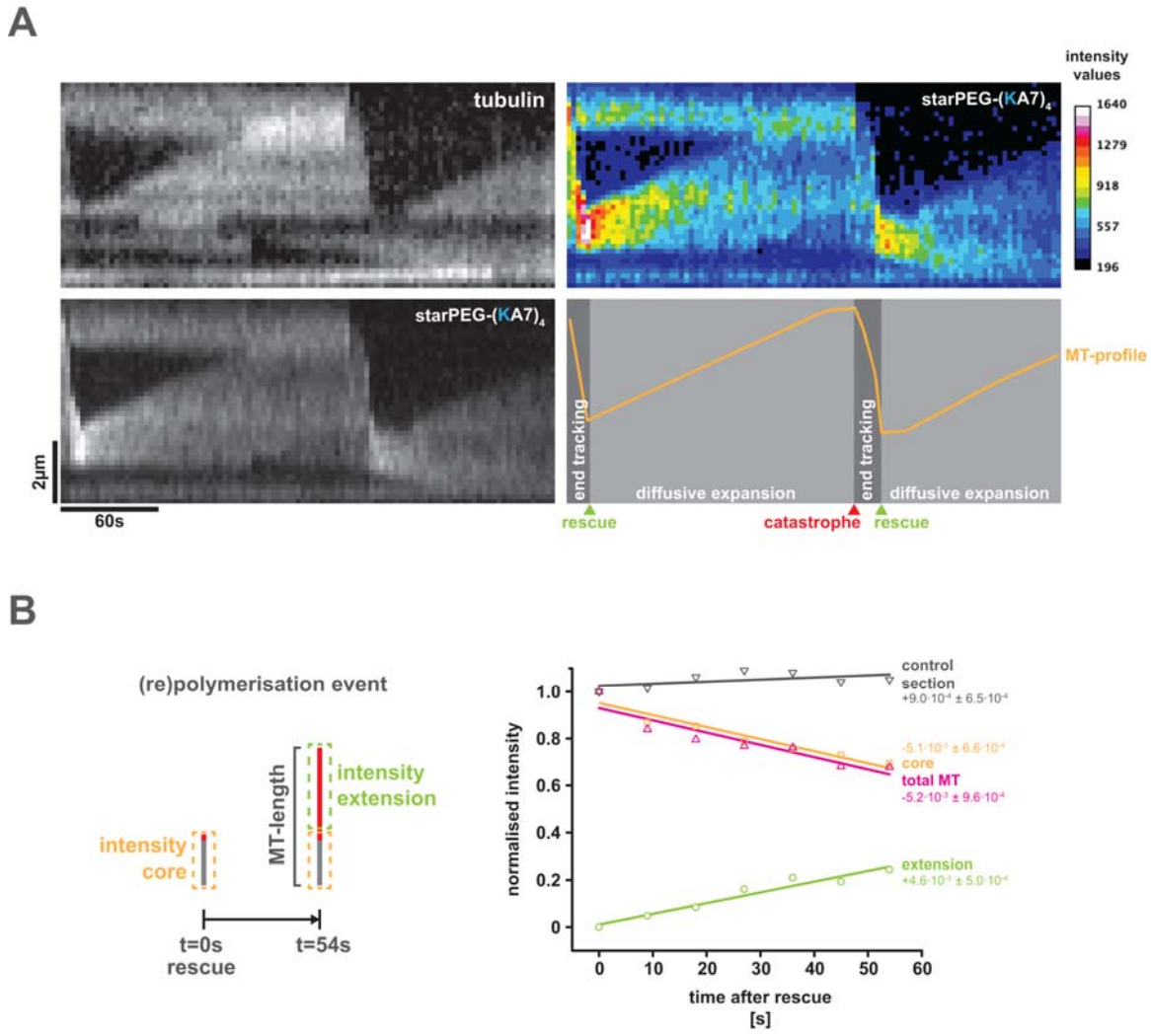
A
tubulin
starPEG-(KA7)4
intensity values
1640
1279
918
557
196
starPEG-(KA7)4
MT-profile
2µm
60s
end tracking
diffusive expansion
end tracking
diffusive expansion
rescue
catastrophe
rescue
B
(re)polymerisation event
intensity core
MT-length
intensity extension
t=0s rescue
t=54s
normalised intensity
time after rescue [s]
control section
+9.0·10-4 ± 6.5·10-4
-5.1·10-3 ± 6.6·10-4
core
total MT
-5.2·10-3 ± 9.6·10-4
extension
+4.6·10-3 ± 5.0·10-4

Figure S5

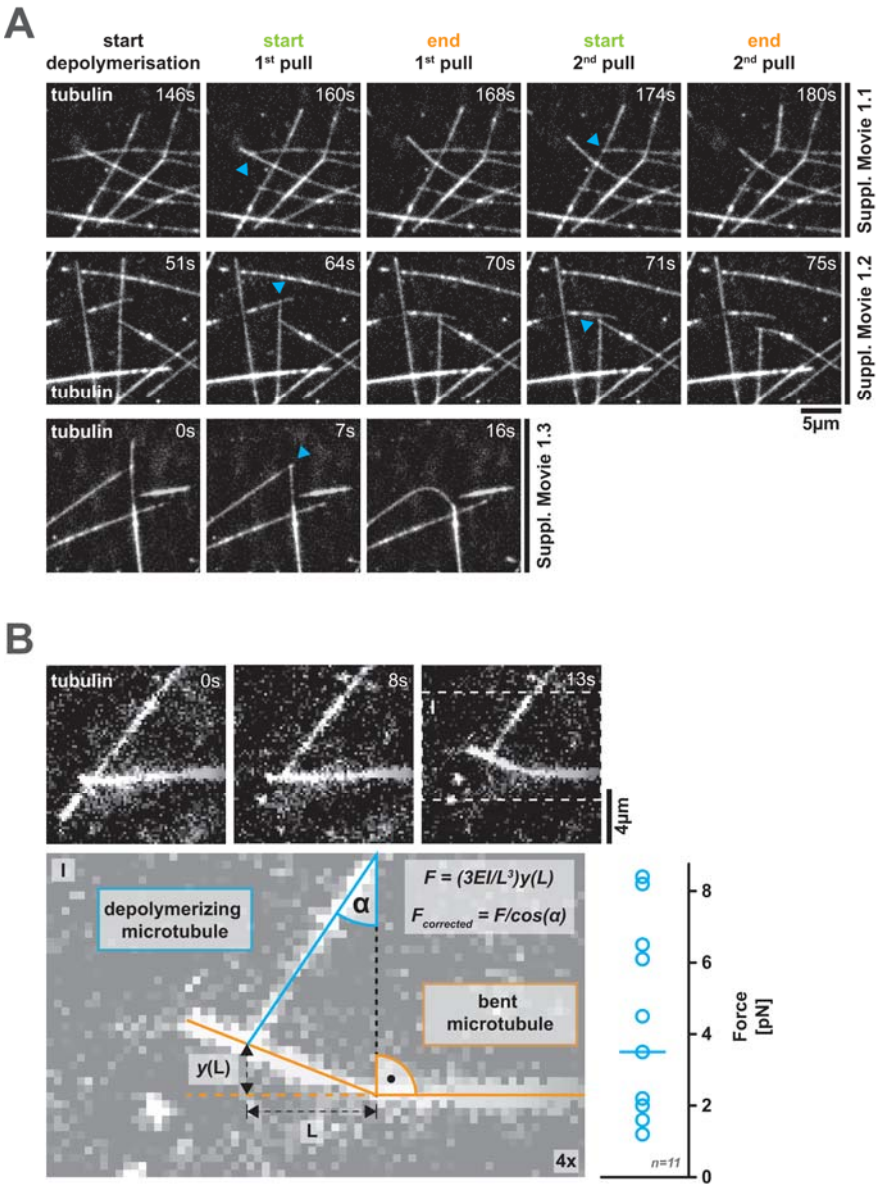
A
start depolymerisation
start 1st pull
end 1st pull
start 2nd pull
end 2nd pull
tubulin
146s
160s
168s
174s
180s
Suppl. Movie 1.1
51s
64s
70s
71s
75s
Suppl. Movie 1.2
5µm
0s
7s
16s
Suppl. Movie 1.3
B
0s
8s
13s
4µm
I
depolymerizing microtubule
α
F = (3EI/L³)y(L)
F corrected = F/cos(α)
bent microtubule
y(L)
L
4x
Force [pN]
n=11

Figure S6

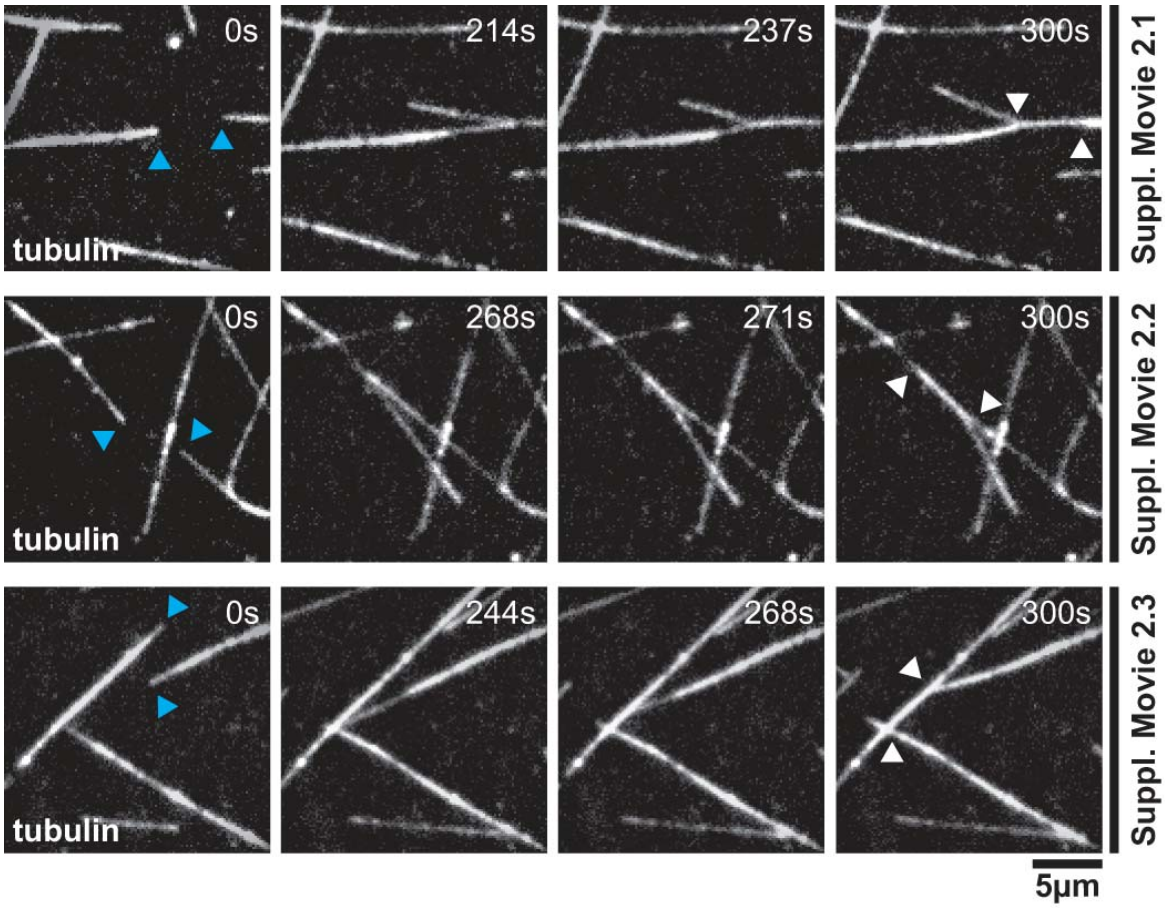
0s
214s
237s
300s
tubulin
Suppl. Movie 2.1
0s
268s
271s
300s
tubulin
Suppl. Movie 2.2
0s
244s
268s
300s
tubulin
Suppl. Movie 2.3
5µm

Figure S7

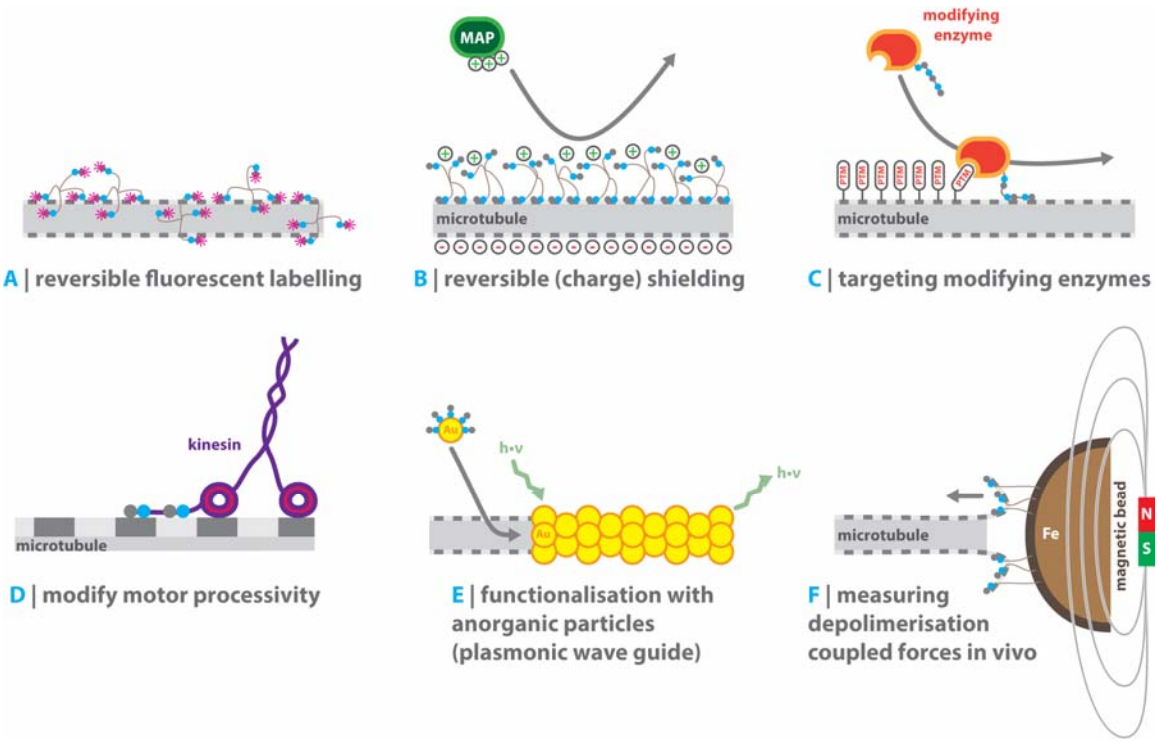
MAP
microtubule
modifying enzyme
microtubule
A | reversible fluorescent labelling
B | reversible (charge) shielding
C | targeting modifying enzymes
kinesin
microtubule
h•v
h•v
microtubule
Fe
magnetic bead
N
S
D | modify motor processivity
E | functionalisation with anorganic particles (plasmonic wave guide)
F | measuring depolimerisation coupled forces in vivo

Figure S8